IRIS AperTO

UNIVERSITÀ DEGLI STUDI DI TORINO

AperTO - Archivio Istituzionale Open Access dell'Università di Torino

Photoenhanced Transformation of Nicotine in Aquatic Environments: Involvement of Naturally Occurring Radical Sources.

This is the author's manuscript

Original Citation:

Availability:

This version is available http://hdl.handle.net/2318/155201 since 2016-10-10T11:11:31Z

Published version:

DOI:10.1016/j.watres.2014.02.016

Terms of use:

Open Access

Anyone can freely access the full text of works made available as "Open Access". Works made available under a Creative Commons license can be used according to the terms and conditions of said license. Use of all other works requires consent of the right holder (author or publisher) if not exempted from copyright protection by the applicable law.

(Article begins on next page)

02 May 2026

UNIVERSITÀ DEGLI STUDI DI TORINO

This Accepted Author Manuscript (AAM) is copyrighted and published by Elsevier. It is posted here by agreement between Elsevier and the University of Turin. Changes resulting from the publishing process - such as editing, corrections, structural formatting, and other quality control mechanisms - may not be reflected in this version of the text. The definitive version of the text was subsequently published in WATER RESEARCH, 55, 2014, http://dx.doi.org/10.1016/j.watres.2014.02.016.

You may download, copy and otherwise use the AAM for non-commercial purposes provided that your license is limited by the following restrictions:

(1) You may use this AAM for non-commercial purposes only under the terms of the CC-BY-NC-ND license.

(2) The integrity of the work and identification of the author, copyright owner, and publisher must be preserved in any copy.

(3) You must attribute this AAM in the following format: Creative Commons BY-NC-ND license (http://creativecommons.org/licenses/by-nc-nd/4.0/deed.en), http://dx.doi.org/10.1016/j.watres.2014.02.016

Photoenhanced transformation of nicotine in aquatic environments: involvement of naturally occurring radical sources.

Monica Passananti[a,b,c], Fabio Temussi[c], Maria Rosaria Iesce[c], Gilles Mailhot[a,b], Davide Vione[d,e], Marcello Brigante[a,b*]

[a] *Clermont Université, Université Blaise Pascal, Institut de Chimie de Clermont-Ferrand (ICCF)- ENSCCF, BP 10448, F-63000 Clermont-Ferrand, France.*

[b] *CNRS, UMR 6296, ICCF, F-63171 Aubière, France*

[c] *UdR Napoli 4 INCA Dipartimento di Scienze Chimiche, Università di Napoli Federico II, Complesso Universitario Monte S. Angelo, Via Cintia, I-80126 Napoli, Italy.*

[d] *Università degli Studi di Torino, Dipartimento di Chimica, Via P. Giuria 5, 10125 Torino, Italy.* http://www.chimicadellambiente.unito.it

[e] *Università degli Studi di Torino, Centro Interdipartimentale NatRisk, Via L. Da Vinci 44, 10095 Grugliasco (TO), Italy.* http://www.natrisk.org

* Corresponding author E-mail: marcello.brigante@univ-bpclermont.fr

Abstract

This work investigated the fate of nicotine (Nico) in aqueous solution upon reaction with singlet oxygen ($^1O_2$) and hydroxyl radical ($HO^\bullet$). The second-order rate constants of Nico with $^1O_2$ ($k_{Nico,\,^1O_2} = (3.38 \pm 0.14) \times 10^6$ M^{-1} s^{-1}) and $HO^\bullet$ ($k_{Nico,\,^\bullet OH} = (1.08 \pm 0.10) \times 10^9$ M^{-1} s^{-1}) were determined using competition kinetics. Photochemical modelling showed that reaction with $HO^\bullet$ would prevail over that with $^1O_2$ as Nico transformation pathway in surface waters. The Nico photochemical half-life times accounted for by the two reactions would vary in the month-year range depending on the environmental conditions: phototransformation would be favoured in shallow water poor in organic matter and rich in nitrate and nitrite. Irradiation experiments of Nico with nitrite suggested that transformation would not be accounted for by $HO^\bullet$ reaction alone. Indeed, a variable fraction of Nico transformation (30-80% depending on the conditions) would take place upon reaction with additional transients, photogenerated NOx being possible candidates. The chemical structures of the transformation intermediates were derived by means of HPLC-MS runs. The detection of nitroderivatives upon irradiation of Nico with nitrite suggests the involvement of nitrogen dioxide in the relevant photoprocesses.

1. Introduction

The fate of pesticides, pharmaceuticals and personal care products (PPCPs) in surface waters is of interest due to their impact on human health and ecosystems (Edwards, 1993; U.S. Environmental Protection Agency). Numerous anthropogenic sources directly emit such compounds in the environment (*i.e.* water and air) and their presence has been extensively reported (Calamari et al., 2003; Garia de Llasera and Bernal-Gonzalez, 2001; Hernando et al., 2006; Kolpin et al., 2002; Schummer et al., 2010; Thomas, 2002).

Recently, particular attention has been devoted to the occurrence of nicotine (Nico) in the environmental compartments. From an atmospheric point of view, the possible formation of indoor aerosol from the heterogeneous chemistry of Nico has been reported (Petrick et al., 2011; Weschler and Fong, 1986). Furthermore, Nico can reach surface waters during tobacco processing and the manufacturing of tobacco products, and concentrations of a few ng L^{-1} have been measured in sewage treatment plants (Martinez Bueno et al., 2011) and in untreated and drinking waters (Illinois Environmental Protection Agency, 2008). Recently, Nico has been found in the main rivers of the Madrid Region in the range of 0.3 – 1.9 μg L^{-1} (Huerta-Fontela et al., 2008; Valcarcel et al., 2011).

Xenobiotics can undergo a variety of abiotic and biological processes in surface waters, including most notably the photochemical reactions. An important issue is that environmental transformation yields intermediates that are sometimes more stable and toxic than the parent compounds (DellaGreca et al., 2003). In addition to direct photolysis, indirect photochemistry can be important and it does not require the relevant pollutants to absorb sunlight. Significant indirect photochemistry pathways involve reactive oxygen species (ROS) such as singlet oxygen ($^1O_2$) and hydroxyl radical ($HO^\bullet$). Singlet oxygen is mainly generated by energy transfer between the triplet states of chromophoric dissolved organic matter (^{3}CDOM*) and ground-state molecular oxygen ($^3O_2$) (Boreen et al., 2003). The $HO^\bullet$ radical can be generated upon irradiation of naturally occurring compounds such as nitrite (NO_2^-), nitrate (NO_3^-) and CDOM. It is the most powerful oxidant occurring in sunlit surface waters, although efficient scavenging by dissolved organic matter limits its steady-state concentrations (Brezonik and Fulkerson-Brekken, 1998). Moreover, the natural occurrence of inorganic nitrogen species such as NO_2^- and NO_3^- can accelerate transformation by photochemically producing nitrogen-centred radicals such as $NO_2^\bullet$, in addition to $HO^\bullet$ (Passananti et al., 2013).

Nicotine was found to be stable under simulated sunlight ($\lambda > 290$ nm) (Boreen et al., 2003). For this reason, in this work we focused on its possible indirect photochemical degradation upon reaction with ROS such as $HO^\bullet$ and $^1O_2$. Particular attention was also focused on Nico phototransformation in the presence of irradiated nitrate and nitrite.

2. Materials and Methods

2.1 Chemicals

Hydrogen peroxide (30 %), sodium carbonate (99.5 %) and sodium nitrate (99 %) were purchased from Fluka; sodium sulphate anhydrous (99.5 %) and sodium nitrite (98%) from Prolabo; nicotine (≥99 %), phosphoric acid (85% in water), sodium chloride (98 %), terephthalic acid (98 %), 2-hydroxyterephthalic acid (97 %), Rose bengal (95%) and furfuryl alcohol (98%) from Sigma Aldrich. All reagents were used as received, without additional purification. All solvents were of HPLC grade and were purchased from Sigma-Aldrich.

Fresh aqueous solutions of nitrate, nitrite or hydrogen peroxide were prepared before each experiment. The concentration of the stock solution of H_2O_2 in milli-Q water was determined using a molar absorption coefficient of 38.1 ± 1.4 M^{-1} cm^{-1} at 240 nm (Miller and Kester, 2002).

2.2 Steady-state irradiation experiments

Nicotine (pK_{a1} = 3.37 ± 0.02, pK_{a2} = 8.07 ± 0.02) (Nienow et al., 2009) in water may be present as neutral, monoprotonated or diprotonated form, depending on pH. In a broad pH range of environmental significance (4.0-7.5), monoprotonated nicotine would be the main species. UV-visible spectra were recorded at different pH values to check for possible variations. Figure 1 reports the absorption spectra of nicotine in aqueous solution at pH 4.7 and 7.7 (showing no differences) and the emission spectrum of the used lamp (solar simulator).

Aqueous solutions were irradiated in a 40 mL thermostated cylindrical reactor, cooled by water circulation at a temperature of 15 ± 2 °C to limit thermal reactions. The reactor was located at one focal point of the lamp to maintain a constant irradiation of the whole sample and it was equipped on top with a Pyrex filter to remove wavelengths lower than ~285 nm. Samples were continuously stirred with a magnetic stirrer and a Teflon bar to ensure homogeneity.

The emission spectrum of the Xenon lamp (see Figure 1) was recorded using a fiber optics coupled with a CCD spectrophotometer (Ocean Optics USD 2000+UV-VIS). A reference lamp (DH-2000-CAL, Ocean Optics) was used for calibration. The irradiance reaching the reactor surface was calculated to be 34 W m^{-2} over the wavelength range 290-400 nm. The adopted intensity was close to the value of 33 W m^{-2} measured between 290 and 400 nm at the "Cézeaux campus" (south of Clermont-Ferrant, France, 45°N Latitude and 3°E Longitude) during a late-summer sunny day at 11:00 am.

2.3 Quantification of hydroxyl radical generation rate

The $HO^\bullet$ formation rate (R^f_{OH}) was determined by using terephthalic acid (TA) as trapping molecule. TA reacts with $HO^\bullet$ leading to the formation of 2-hydroxyterephthalic acid

(TAOH) with a yield (Y_{TAOH}) determined as the ratio between the initial formation rate of TAOH (R^f_{TAOH}) and the initial degradation rate of TA (R^d_{TA}). Y_{TAOH} ranged between 12% and 30%, depending on the pH and temperature of aqueous media (Charbouillot et al., 2011). This method enables a simple and fast measurement of photogenerated $HO^\bullet$, with a high sensitivity that allows detection of steady-state concentration values below 10^{-18} M.

To calculate the formation rate of $HO^\bullet$ as a function of the composition of different aqueous media, different solutions were irradiated with the same setup described in Passananti et al. (2013). An aliquot of solution (3 mL) was withdrawn from the reactor and put in a fluorescence cuvette at fixed times. The cuvette was transferred into a Perkin-Elmer MPF 3 L spectrofluorimeter and TAOH was quantified (λ_{ex} = 320 nm, λ_{em} = 420 nm) by using a calibration curve previously made with standard solutions of TAOH. The concentration of TA in all the experiments was included between 500 µM and 1 mM to trap all photogenerated $HO^\bullet$.

2.4 Kinetic study: hydroxyl radical and singlet oxygen

The second-order reaction rate constant between *i*) nicotine and hydroxyl radical ($k_{Nico,\,^\bullet OH}$) and *ii*) nicotine and singlet oxygen ($k_{Nico,\,^1O_2}$) were determined using a competition method. The time trends of Nico and of the reference compounds (TA for $HO^\bullet$ and FFA for $^1O_2$) were monitored upon irradiation of H_2O_2 ($HO^\bullet$ source) and Rose Bengal ($^1O_2$ source). Irradiation of H_2O_2, Nico and TA was carried out with the polychromatic irradiation system described in section 2.2. Sample aliquots were withdrawn at selected time intervals and the time trend of Nico and TA was monitored by liquid chromatography.

For $^1O_2$ generation, a xenon lamp equipped with a Pyrex filter and a monochromator was used to selectively irradiate Rose Bengal (20 µM in aqueous solution) at 540 nm. To determine the second-order rate constant between $^1O_2$ and Nico ($k_{Nico,\,^1O_2}$) by competition kinetics with FFA, the solution was put in a quartz cuvette (3 mL) and irradiated. Aliquots of 100 µL were withdrawn at fixed time intervals and analysed by liquid chromatography.

2.5 Photoinduced degradation and data analysis.

All experiments were performed in Milli-Q water and pH was adjusted using NaOH or $HClO_4$. Hydrogen peroxide, nitrate or nitrite were added just before irradiation to a constant concentration of Nico (25 µM). Degradation was monitored by liquid chromatography.

An HPLC system (Waters Alliance) equipped with a diode array detector was used for analysis of Nico, FFA and TA. An Eclipse XDB-C18 column (Agilent, 4.6 x 150 mm, 5 µm) and an isocratic method was adopted, using 98% acidified water (0.5% formic acid) and 2% methanol. The flow rate was 0.6 mL min^{-1} and the retention time of nicotine was 4 min. For FFA the method was 90% water and 10% acetonitrile, flow rate 1 mL min^{-1} and retention

time of 4.3 min. TA was eluted and quantified as previously described by Charbouillot et al. (2011).

The time evolution of Nico in the presence of the photogenerated oxidant species was fitted with a pseudo-first order equation of the type: $\frac{[Nico]_t}{[Nico]_0} = \exp(-kt)$, where $[Nico]_0$ and $[Nico]_t$ are nicotine concentrations (initial and at time *t*, respectively) and *k* is the pseudo-first order degradation rate constant. The error bars associated to the rate data represent 3σ, derived from the scattering of the experimental data around the fit curves (intra-series variability).

2.6 Phototransformation products identification

In a typical procedure to identify degradation products, 200 μM of Nicotine were irradiated in the presence of: (*i*) hydrogen peroxide 700 μM; (*ii*) nitrate 300μM and (*iii*) nitrite 100μM, up to 50% degradation of initial Nico. Experiments were performed under the same irradiation conditions as the degradation experiments described before.

An LC-MS system (Agilent 1100 Series, binary pump) equipped with an ESI ion source (MSD VL) was adopted to identify Nico degradation products. The column was a Sphere Clone C18 (Phenomenex, 4.6 x 250 mm, 5 μm) and the following gradient elution was used: at the initial time, 5% acetonitrile and 95% water (acidified with 1% formic acid), followed by a linear gradient to 75% acetonitrile within 55 min. The 75% acetonitrile ratio was then maintained constant for 20 min. The flow rate was 0.4 mL min^{-1}. Degradation products identification was performed on the basis of previously reported literature on the Nicotine transformation and radical driven reactivity as reported in Section 3.3.

2.7. Photochemical modelling

Based on the second-order reaction rate constants with $HO^{\bullet}$ and $^1O_2$ determined experimentally, the transformation half-life time of Nico *via* the two photochemical processes was modelled as a function of water chemistry and depth. The used model approach has been validated against available data of pollutant photodegradation in the field (Maddigapu et al., 2011; Vione et al., 2011; De Laurentiis et al., 2012).

Recently, a software application has been derived from the model (APEX: Aqueous Photochemistry of Environmentally-occurring Xenobiotics; Vione, in press). It is available for free download at *http://chimica.campusnet.unito.it/do/didattica.pl/Quest?corso=7a3d*, including the User's Guide that contains a comprehensive account of model equations. APEX uses photochemical reactivity parameters as input data (direct photolysis quantum yields and reaction rate constants with reactive transients) and it models (among others) half-life times and pseudo-first order phototransformation rate constants as a function of water chemistry and depth. As time unit for the output APEX uses a Summer Sunny Day (SSD), which corresponds to fair-weather 15 July at 45°N latitude. As far as depth is concerned, the model actually considers the path length *l* of sunlight in water. The path length is longer than the

depth *d* because sunlight does not penetrate vertically in water, although refraction deviates the light path towards the vertical. On 15 July at 45°N it is $l = 1.05\ d$ at noon and $l = 1.17\ d$ at ±3 h from noon, a correction that is smaller than the uncertainty associated with the model (Vione, in press). A full seasonal trend of *l vs. d* is provided in the User's Guide of APEX. Finally, APEX applies to well-mixed surface water layers and the output quantities are water-column averages. Therefore, by fixing $l = 1$ m, the output values (half-life times or pseudo-first order rate constants) are averages over the 1-m water column and not the point values at 1 m path length.

3. Results and Discussion

3.1 Second-order rate constants with $HO^\bullet$ and $^1O_2$

First of all, the second-order kinetic constants of nicotine with $^1O_2$ and $HO^\bullet$ were determined by use of Rose Bengal and H_2O_2 as respective ROS sources. Competition kinetics was exploited, between Nico and TA in the case of $HO^\bullet$ (R1 and R2) and between Nico and FFA for $^1O_2$ (R3 and R4).

$Nico + HO^\bullet \rightarrow products_1$ $\quad k_{Nico,\ HO^\bullet}$ (R1)

$TA + HO^\bullet \rightarrow products_2$ $\quad k_{TA,\ HO^\bullet} = 4.0\times10^9\ M^{-1}s^{-1}$ (Charbouillot et al., 2011) (R2)

$Nico + {}^1O_2 \rightarrow products_1$ $\quad k_{Nico,\ ^1O_2}$ (R3)

$FFA + {}^1O_2 \rightarrow products_2$ $\quad k_{FFA,\ ^1O_2} = 1.2\times10^8\ M^{-1}s^{-1}$ (Haag et al., 1984) (R4)

In either system, the competitive reaction treatment gives:

$$\ln\frac{[Nico]_0}{[Nico]_t} = \frac{k_{Nico,\ ox}}{k_{Ref,\ ox}}\ln\frac{[Ref]_0}{[Ref]_t}$$

where *ox* is the oxidant ($^1O_2$ or $HO^\bullet$) and *Ref* is the reference compound (FFA or TA). The slope of the linear plots reported in Figure 2 gives the second-order rate constants $k_{Nico,\ ^1O_2} = (3.38 \pm 0.14) \times 10^6\ M^{-1}\ s^{-1}$ and $k_{Nico,\ ^\bullet OH} = (1.08 \pm 0.10) \times 10^9\ M^{-1}\ s^{-1}$.

3.2 Irradiation in the presence of nitrite, nitrate and hydrogen peroxide

Nitrite, nitrate and hydrogen peroxide were varied over a large range of concentrations and the rates of $HO^\bullet$ formation and Nico degradation were determined in each case. Figure 3A reports the degradation rates of Nico as a function of different concentrations of $HO^\bullet$ sources. As expected, a linear correlation was found between R^d_{Nico} and the concentrations of nitrate and H_2O_2: $R^d_{Nico} = (9.7 \pm 1.5) \times 10^{-9}\ [NO_3^-]$ and $R^d_{Nico} = (1.4 \pm 0.2) \times 10^{-7}\ [H_2O_2]$.

Interestingly, in the presence of nitrite, the degradation rate of Nico reached a maximum around 30 µM NO_2^- ($R^d_{Nico} \sim 3 \times 10^{-11}$ M s^{-1}) and decreased down to 0.9×10^{-11} M s^{-1} in the presence of 50 µM NO_2^- (Figure 3B). Such trend is difficult to be explained by only taking the $HO^\bullet$ reactivity into account.

With 25 µM Nico and nitrite in the 10-50 µM range, only a limited fraction of photogenerated $HO^\bullet$ reacts with Nico (from 5 to 20%, using $k_{NO_2^-, {}^\bullet OH} = 1.1 \times 10^{10}$ M^{-1} s^{-1} (Buxton et al., 1988) and $k_{Nico, {}^\bullet OH} = (1.08 \pm 0.10) \times 10^9$ M^{-1} s^{-1}). Such a reaction would account for 20-70% of Nico degradation, depending on the conditions. Most $HO^\bullet$ would be scavenged by nitrite leading to the formation of $NO_2^\bullet$. Photogenerated $NO_2^\bullet$ can react with electron-rich aromatic rings (*e.g.* phenol, Vione et al. (2004)), contributing to the degradation of pollutants.

Doubtless, the mechanism of nitrite and nitrate photolysis is complex and there is still uncertainty about the primary photoprocesses and subsequent reactions (Mark et al., 1996). For instance, generation of dinitrogen tetroxide (N_2O_4) and dinitrogen trioxide (N_2O_3) could represent a possible sink of photogenerated radicals ($NO_2^\bullet$ and $NO^\bullet$, the latter produced in nitrite photolysis along with $HO^\bullet$). However, it could also represent a source of reactive species (nitrating and/or nitrosating agents; Beitz et al., 1999).

3.3 Degradation pathways

Different degradation products were identified using ESI detection. Products **2** (a, b and c), **5** and **6** were commonly found in the presence of hydrogen peroxide or nitrite, while products **3** and **4** were detected only in nitrite solution. In Fig. 4 the possible reaction mechanism between Nico and photogenerated hydroxyl radical is reported also on the basis of literature data (Parsons, 2000b). The first step is the hydrogen abstraction that could lead to the formation of a resonance-stabilized radical intermediate (step 1). Subsequently, two possible pathways are suggested: i) reactivity with photogenerated hydroxyl radical (step 2) leading to the formation of hydroxylated Nico derivatives with $[M + H]^+$ = 179 m/z and ii) reaction with dissolved oxygen leading to the formation of a peroxide intermediate (step 3). Formation of nitroderivatives (**3** and **4**, $[M + H]^+$ = 224 and 240 m/z) could be explained by hydrogen shift from an oxygenated intermediate (Parsons, 2000b). Moreover, ringbreaking with ketone formation is a possible evolution of the peroxide radical precursor of compound **5** ($[M + H]^+$ = 179m/z) (Parsons, 2000a).

Hydroxyl radical could also generate the radical in position 2 on the pyrrolidine ring (Fig. 5), followed by the formation of hydroxylated Nico **2c** ($[M + H]^+$ = 179 m/z) (via $HO^\bullet$) and cotinine **6** ($[M + H]^+$ = 177 m/z) (via O_2). In the presence of nitrite, the increase of Nico degradation could be explained by the reactivity of $NO_x^\bullet$ on the radical intermediates leading to the formation of nitrous derivative (Akhtar and Pechet, 1964; Barton et al., 1960) that

tautomerizes to oxime. Under adopted experimental conditions the oxime is easly hydrolyzed to **6**.

3.4 Environmental lifetime calculations

Considering that direct photodegradation of Nico is negligible under sun-simulated conditions, the possible fate toward hydroxyl radical and singlet oxygen could be predicted. The reverse of the total half-life time is given by the sum of the reciprocal half-life time for each reaction (eq. 1):

$$\frac{1}{T_{1/2}} = \frac{1}{\tau_{1/2}(HO^{\bullet})} + \frac{1}{\tau_{1/2}(^1O_2)} \qquad \text{eq 1}$$

Where $\tau_{1/2}(HO^{\bullet})$ and $\tau_{1/2}(^1O_2)$ are the half-life time of Nico in the presence of $HO^{\bullet}$ and $^1O_2$ respectively.

Equation 1 could be rearranged to:

$$T_{1/2} = \frac{\tau_{1/2}(HO^{\bullet}) \times \tau_{1/2}(^1O_2)}{\tau_{1/2}(HO^{\bullet}) + \tau_{1/2}(^1O_2)} \qquad \text{eq 2}$$

The total half-life time of Nico ($T_{1/2}$) has been reported in Figure 6 as a function of an environmental steady-state concentration range of hydroxyl radical $[HO^{\bullet}]_{ss}$ and singlet oxygen $[^1O_2]_{ss}$. The values range *i*) from 10^{-17} M up to 5×10^{-16} M for $HO^{\bullet}$ and *ii*) from 5×10^{-15} M up to 10^{-13} M $^1O_2$ (Brezonik and Fulkerson-Brekken, 1998; Haag and Hoigne, 1986; Russi et al., 1982; Vione et al., 2010).

The photochemical half-life time $t_{½}$ of Nico in surface waters upon reaction with $HO^{\bullet}$ and $^1O_2$ was modelled by using the *Plotgraph* function of APEX. Figure 7 reports $t_{½}$ as a function of dissolved organic carbon (DOC, which is a measure of dissolved organic matter, DOM) and of the optical path length *l* of sunlight in water. The half-life time varies from around one month to almost an year and it increases with both DOC and *l*. The increase with *l* is accounted for by the fact that deeper water bodies are less thoroughly illuminated by sunlight, in particular as far as their bottom layers are concerned. To account for the increase with DOC, one should consider that most of Nico transformation would take place upon reaction with $HO^{\bullet}$, while $^1O_2$ would only play a secondary role. High DOC means both high DOM and high CDOM but, while CDOM is a photochemical $HO^{\bullet}$ source (Vione et al., 2010), DOM is often a more important $HO^{\bullet}$ scavenger. Therefore, $HO^{\bullet}$-induced reactions usually occur to a higher extent in low-DOC waters (Brezonik and Fulkerson-Brekken, 1998).

Contrary to $HO^{\bullet}$, the importance of $^1O_2$ increases with increasing DOC because singlet oxygen is produced by reaction of the triplet states ^{3}CDOM* with O_2. Actually, high DOC enhances both ^{3}CDOM* and $^1O_2$. However, for $^1O_2$ to play an important role in Nico transformation one would need DOC around 10 mg C L^{-1}, under which circumstances the

photochemical half-life time would be in the range of years. In this case, it is very likely that other transformation processes would prevail over reactions with $^1O_2$ or $HO^\bullet$.

Due to the importance of reaction with $HO^\bullet$, Nico phototransformation would understandably be enhanced by increasing nitrate and nitrite (photochemical $HO^\bullet$ sources), as shown in Figure 8 (remember that faster transformation leads to lower $t_{½}$). Overall, the predicted photochemical half-life times of Nico in surface waters are relatively high (month-year range). This is caused by the relatively low reaction rate constant with $HO^\bullet$ (about one order of magnitude lower than the limit of diffusive control; Buxton et al., 1988) and by the secondary role of $^1O_2$. However, other photochemical pathways could be potentially important for Nico. For instance, APEX data suggest that transformation by ^{3}CDOM* could be significant in high-DOC waters, if the reaction rate constant of Nico with triplet states was in the order of 10^8 M^{-1} s^{-1}.

4. Conclusions

The degradation of nicotine was investigated in the presence of different naturally occurring photochemical sources of $HO^\bullet$ and of nitrogen-centered radicals. The second-order kinetic constants of nicotine with $HO^\bullet$ and $^1O_2$ were determined, which allowed a prediction of the environmental half-life times for such reactions as a function of water chemistry and depth. Photochemical modeling showed that $HO^\bullet$ would prevail over $^1O_2$ as reactive species for Nico photodegradation. The relevant half-life times in surface waters would vary in the month-year range, depending on environmental conditions. Nico transformation is favoured by elevated nitrate and nitrite and inhibited in deep or DOM-rich waters. Due to the relatively slow transformation kinetics with $HO^\bullet$ in high-DOC conditions, there is the possibility for other photoreactants (*e.g.* ^{3}CDOM*) to play a significant role in the degradation of Nico.

Laboratory experiments with irradiated nitrite suggested that additional reactive species such as nitrogen oxides could be involved in Nico phototransformation, which was not fully accounted for by $HO^\bullet$ produced by nitrite photolysis. Involvement of nitrogen-centered radicals in the photochemical transformation of Nico is supported by the detection of nitroderivatives as transformation intermediates upon irradiation of nitrite. The formation of nitroderivatives by irradiation of xenobiotics in presence of nitrite and nitrate has been previously observed (Shankar et al., 2007) and the formation of NO- and NO_2-phenyl substituted compounds was explained by reaction with $NO^\bullet$ and $NO_2^\bullet$ (Nélieu et al., 2004). These reactions are environmentally significant and, for instance, photonitration has been observed in natural waters and found to yield nitroderivatives of phenolic pesticides (Chiron et al., 2007). Photonitration leads in many cases to the formation of compounds that are

environmentally more persistent and more toxic than the parent molecules (Chiron et al., 2009; Suzuki et al., 1982).

To have a better estimate of the environmental degradation rate of Nico, it would be important to study its reactivity toward reactive nitrogen species that may be present in natural waters. Moreover, it would be very important to understand the interaction of Nico with other naturally occurring species and to study the stability and toxicity of its environmental metabolites.

References

Akhtar, M., Pechet, M.M., 1964. The mechanism of the Barton reaction. J. Am. Chem. Soc. 86, 265-268.

Barton, D.H.R., Beaton, J.M., Geller, L.E., Pechet, M.M., 1960. A new photochemical reaction. J. Am. Chem. Soc. 82, 2640-2641.

Beitz, T., Bechmann, W., Mitzner, R. Investigation of the photoreactions of nitrate and nitrite ions with selected azaarenes in water. Chemosphere 1999, 38, 351-361.

Boreen AL, Arnold WA, McNeill K. Photodegradation of pharmaceuticals in the aquatic environment: A review. Aquat Sci 2003;65:320-41.

Brezonik PL, Fulkerson-Brekken J. Nitrate-induced photolysis in natural waters: controls on concentrations of hydroxyl radical photo-intermediates by natural scavenging agents. Environ Sci Technol 1998; 32: 3004-3010.

Buxton, G.V., Greenstock, C.L., Phillips Helman, W., Ross, A.B., 1988. Critical review of rate constants for reactions of hydrated electrons, hydrogen atoms and hydroxyl radicals (°OH/°O-) in aqueous solution. J. Phys. Chem. Ref. Data 17, 513-886.

Calamari D, Zuccato E, Castiglioni S, Bagnati R, Fanelli R. Strategic Survey of Therapeutic Drugs in the Rivers Po and Lambro in Northern Italy. Environ Sci Technol 2003; 37: 1241-1248.

Charbouillot T, Brigante M, Mailhot G, Maddigapu PR, Minero C, Vione D. Performance and selectivity of the terephthalic acid probe for ·OH as a function of temperature, pH and composition of atmospherically relevant aqueous media. J Photochem Photobiol, A 2011; 222: 70-76.

Chiron S, Comoretto L, Rinaldi E, Maurino V, Minero C, Vione D. Pesticide by-products in the Rhône delta (Southern France). The case of 4-chloro-2-methylphenol and of its nitroderivative. Chemosphere 2009; 74: 599-604.

Chiron S, Minero C, Vione D. Occurrence of 2,4-Dichlorophenol and of 2,4-Dichloro-6-Nitrophenol in the RhÃ´ne River Delta (Southern France). Environ Sci Technol 2007; 41: 3127-3133.

De Laurentiis E, Chiron S, Kouras-Hadef S, Richard C, Minella M, Maurino V, Minero C, Vione D. Photochemical fate of carbamazepine in surface freshwaters: Laboratory measures and modelling. Environ Sci Technol 2012;46:8164-73.

DellaGreca M, Brigante M, Isidori M, Nardelli A, Previtera L, Rubino M, et al. Phototransformation and ecotoxicity of the drug Naproxen-Na. Environ Chem Lett 2003; 1: 237-241.

Edwards CA. The Impact of pesticides on the environment. In: Pimentel D, Lehman H, editors. The Pesticide Question. Springer US, 1993, pp. 13-46.

Garia de Llasera MP, Bernal-Gonzalez M. Presence of carbamate pesticides in environmental waters from the northwest of Mexico: determination by liquid chromatography. Water Res 2001; 35: 1933-1940.

Haag WR, Hoigne J. Singlet oxygen in surface waters. 3. Photochemical formation and steady-state concentrations in various types of waters. Environ Sci Technol 1986; 20: 341-348.

Haag WR, Hoigne J, Gassman E, Braun AAM. Singlet oxygen in surface waters - Part I: Furfuryl alcohol as a trapping agent. Chemosphere 1984; 13: 631-640.

Hernando MD, Mezcua M, Fernandez-Alba AR, Barcelo D. Environmental risk assessment of pharmaceutical residues in wastewater effluents, surface waters and sediments. Talanta 2006; 69: 334-342.

Huerta-Fontela M, Galceran MT, Martin-Alonso J, Ventura F. Occurrence of psychoactive stimulatory drugs in wastewaters in north-eastern Spain. Sci Total Environ 2008; 397: 31-40.

Illinois Environmental Protection Agency. Report on pharmaceuticals and personal care products in Illinois drinking water. http://www.epa.state.il.us/water/pharmaceuticals-in-drinking-water.pdf, 2008.

Kolpin DW, Furlong ET, Meyer MT, Thurman EM, Zaugg SD, Barber LB, et al. Pharmaceuticals, hormones, and other organic wastewater contaminants in U.S. streams, 1999-2000: a national reconnaissance. Environ Sci Technol 2002; 36: 1202-1211.

Maddigapu PR, Minella M, Vione D, Maurino V, Minero C. Modeling phototransformation reactions in surface water bodies: 2,4-Dichloro-6-nitrophenol as a case study. Environ Sci Technol 2011;45:209-14.

Mark G, Korth H-G, Schuchmann H-P, von Sonntag C. The photochemistry of aqueous nitrate ion revisited. J Photochem Photobiol, A 1996; 101: 89-103.

Martinez Bueno MJ, Ucles S, Hernando MD, Davoli E, Fernandez-Alba AR. Evaluation of selected ubiquitous contaminants in the aquatic environment and their transformation products. A pilot study of their removal from a sewage treatment plant. Water Res 2011; 45: 2331-2341.

Miller WL, Kester DR. Hydrogen peroxide measurement in seawater by (p-hydroxyphenyl)acetic acid dimerization. Anal Chem 2002; 60: 2711-2715.

Nélieu S, Kerhoas L, Sarakha M, Einhorn J. Nitrite and nitrate induced photodegradation of monolinuron in aqueous solution. Environ Chem Lett 2004; 2: 83-87.

Nienow AM, Hua I, Poyer IC, Bezares-Cruz JC, Jafvert CT. Multifactor statistical analysis of H_2O_2-enhanced photodegradation of nicotine and phosphamidon. Ind. Eng. Chem. Res. 2009; 48: 3955–3963.

Parsons, A.F., 2000a. An Introduction to Free Radical Chemistry (Chapter 4). Blackwell Sciences Ltd.

Parsons, A.F., 2000b. An Introduction to Free Radical Chemistry (Chapter 9). Blackwell Sciences Ltd.

Passananti M, Temussi F, Iesce MR, Mailhot G, Brigante M. The impact of the hydroxyl radical photochemical sources on the rivastigmine drug transformation in mimic and natural waters. Water Res 2013; 47: 5422-5430.

Petrick LM, Svidovsky A, Dubowski Y. Thirdhand Smoke: Heterogeneous Oxidation of Nicotine and Secondary Aerosol Formation in the Indoor Environment. Environ Sci Technol 2011; 45: 328-333.

Russi H, Kotzias D, Korte F. Photoinduzierte hydroxylierungsreaktionen organischer chemikalien in naturlichen Gewassern - Nitrate als potentielle OH-radikalquellen. Chemosphere 1982; 11: 1041-1048.

Schummer C, Mothiron E, Appenzeller BMR, Rizet A-L, Wennig R, Millet M. Temporal variations of concentrations of currently used pesticides in the atmosphere of Strasbourg, France. Environ Pollut 2010; 158: 576-584.

Shankar MV, Nélieu S, Kerhoas L, Einhorn J. Photo-induced degradation of diuron in aqueous solution by nitrites and nitrates: Kinetics and pathways. Chemosphere 2007; 66: 767-774.

Suzuki J, Okazaki H, Nishi Y, Suzuki S. Formation of mutagens by photolysis of aromatic compounds in aqueous nitrate solution. Bull Environ Contam Toxicol 1982; 29: 511-516.

Thomas H. Occurrence, fate, and removal of pharmaceutical residues in the aquatic environment: a review of recent research data. Toxicol Lett 2002; 131: 5-17.

U.S. Environmental Protection Agency. Pesticides: Health and Safety, http://www.epa.gov/opp00001/health/human.htm.

Valcarcel Y, Gonzalez Alonso S, Rodriguez-Gil JL, Gil A, Catala M. Detection of pharmaceutically active compounds in the rivers and tap water of the Madrid Region (Spain) and potential ecotoxicological risk. Chemosphere 2011; 84: 1336-1348.

Vione D, Bagnus D, Maurino V, Minero C. Quantification of singlet oxygen and hydroxyl radicals upon UV irradiation of surface water. Environ Chem Lett 2010; 8: 193-198.

Vione D, Maurino V, Minero C, Pelizzetti E. Phenol nitration upon oxidation of nitrite by Mn(III,IV) (hydr)oxides. Chemosphere 2004; 55: 941-949.

Vione D, Maddigapu PR, De Laurentiis E, Minella M, Pazzi M, Maurino V, Minero C, Kouras S, Richard C. Modelling the photochemical fate of ibuprofen in surface waters. Wat Res 2011;45:6725-36.

Vione D. A test of the potentialities of the APEX software (Aqueous Photochemistry of Environmentally occurring Xenobiotics). Modelling the photochemical persistence of the herbicide cycloxydim in surface waters, based on literature kinetic data. Chemosphere, in press. DOI: 10.1016/j.chemosphere.2013.10.078.

Weschler CJ, Fong KL. Characterization of organic species associated with indoor aerosol particles. Environment International 1986; 12: 93-97.

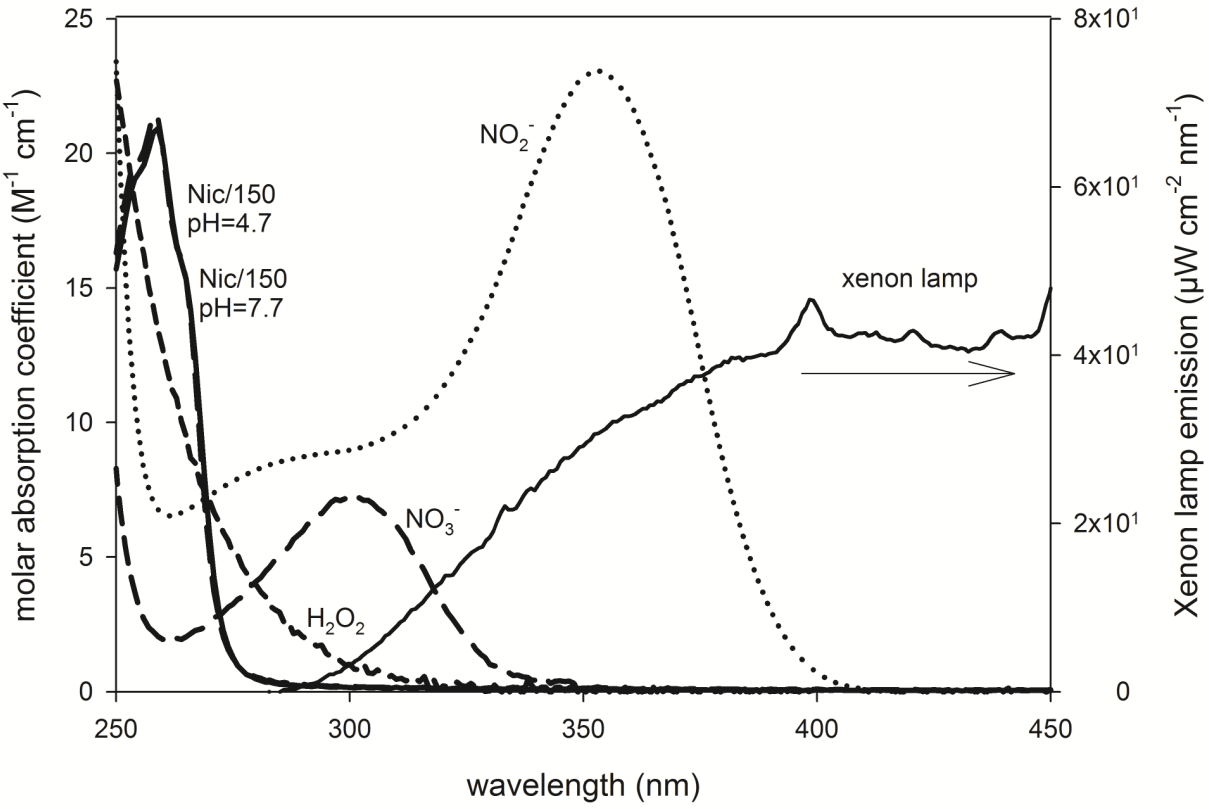

Figure 1: Emission spectrum reaching the solution and molar absorption coefficients of the aqueous nicotine (at pH 4.7 and 7.7), nitrate, nitrite and H_2O_2.

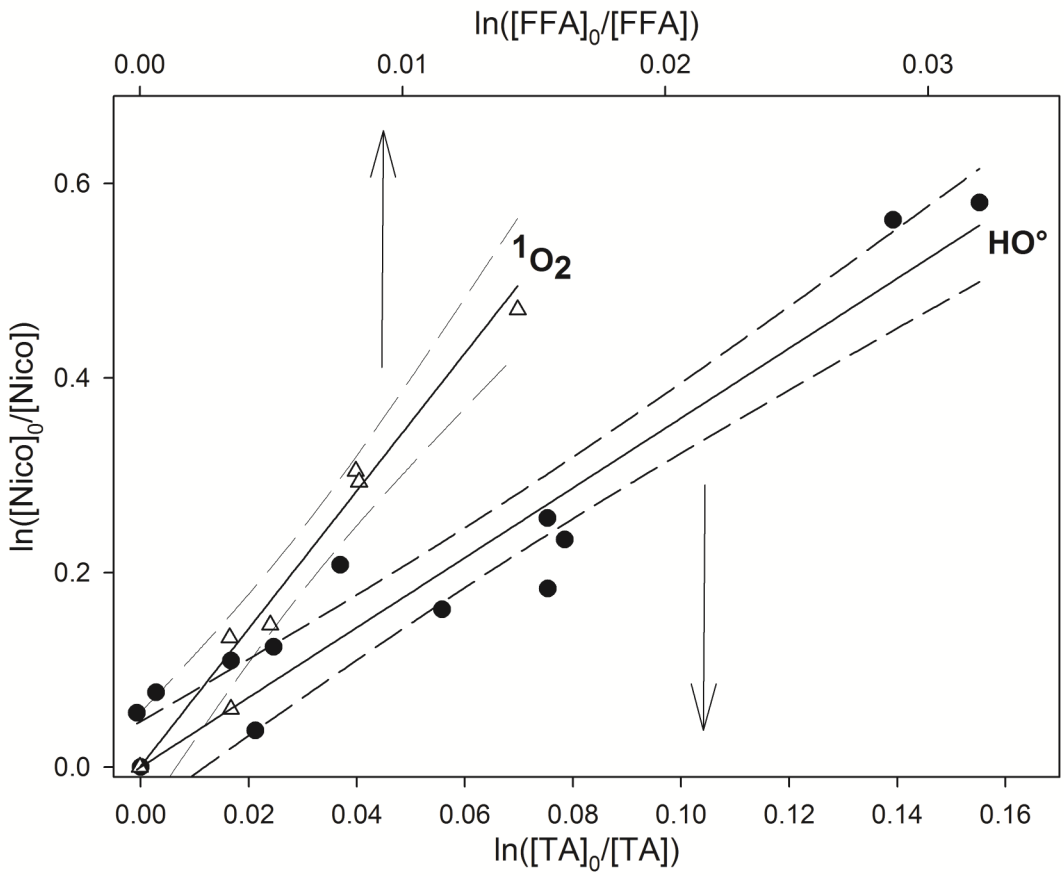

Figure 2: Plot of $\ln([TA]_0/[TA])$ *vs* $\ln([Nico]_0/[Nico])$ and $\ln([FFA]_0/[FFA])$ *vs* $\ln([Nico]_0/[Nico])$ for the decay of Terephthalic acid (TA) and Nicotine (Nico) during the photolysis of H_2O_2 (350 µM) (●) and Furfuryl alcool (FFA) and Nicotine (Nico) during the photolysis of Rose Bengal (20 µM) (Δ). Experiments were performed at 15 ± 2 °C. Dashed lines denote the 95% confidence of the linear fit.

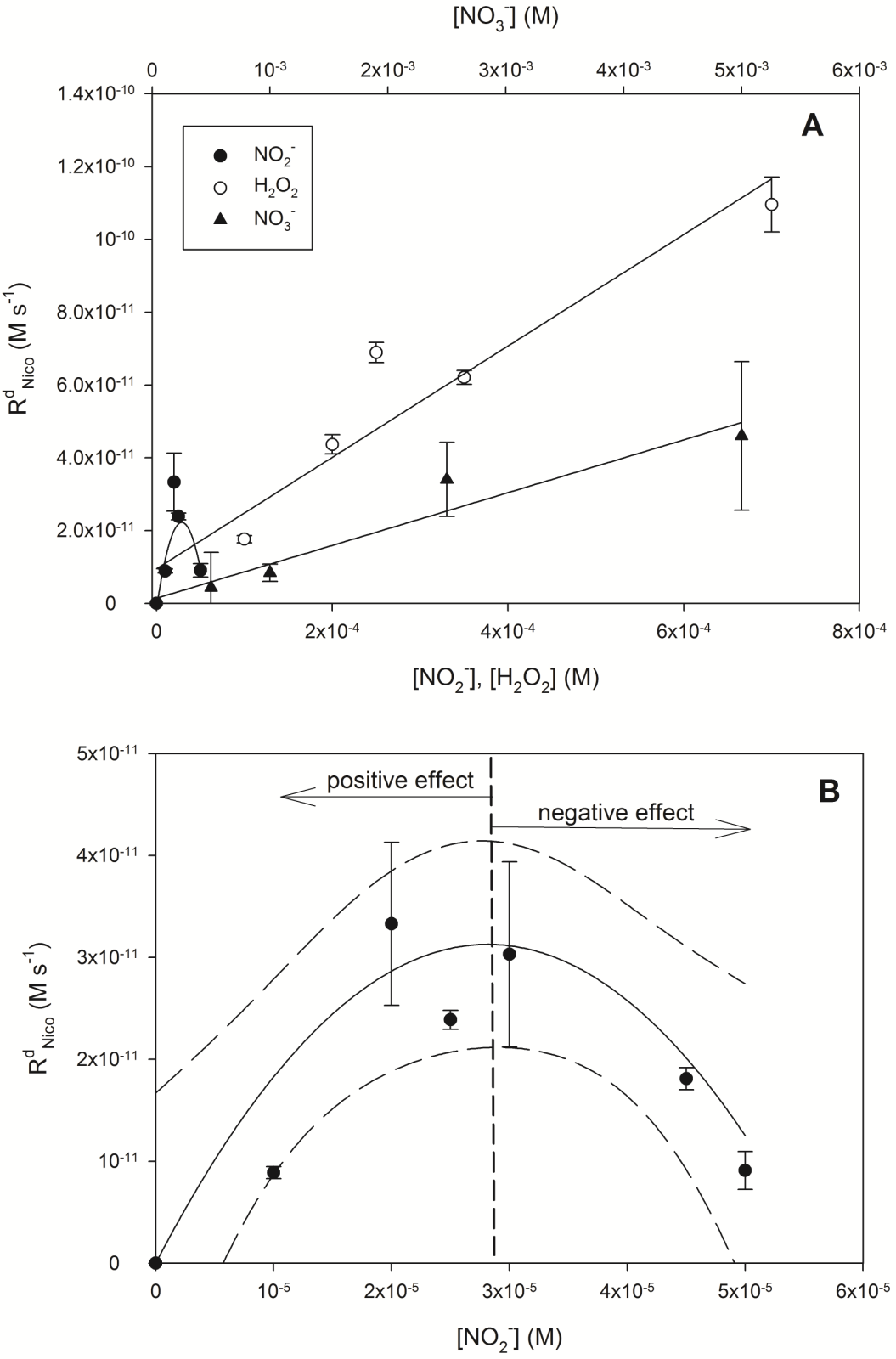

Figure 3: **A**) Correlation between the initial degradation rate of nicotine R^{d}_{Nico}(M s^{-1}) and concentration of nitrite (●) hydrogen peroxide (○) and nitrate (▲). **B**) R^{d}_{Nico}(M s^{-1}) as a function of nitrite concentration. The errors bars represent the 3σ based on the linear fit of experimental data. Dashed lines denote the 95% confidence of the linear fit.

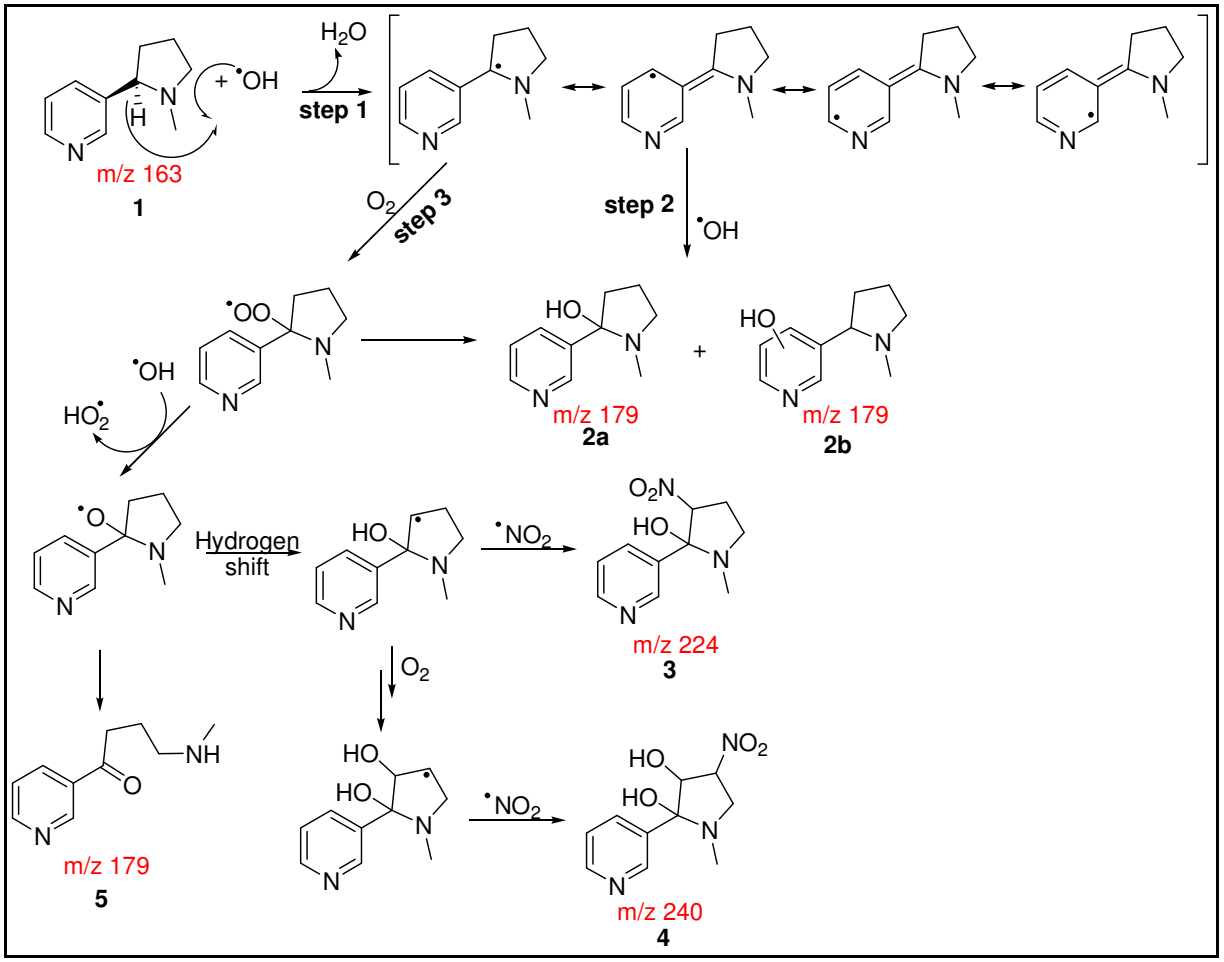

Figure 4: First proposed reaction mechanism between Nico and photogenerated hydroxyl radical with first hydrogen and formation of a resonance-stabilized radical intermediate.

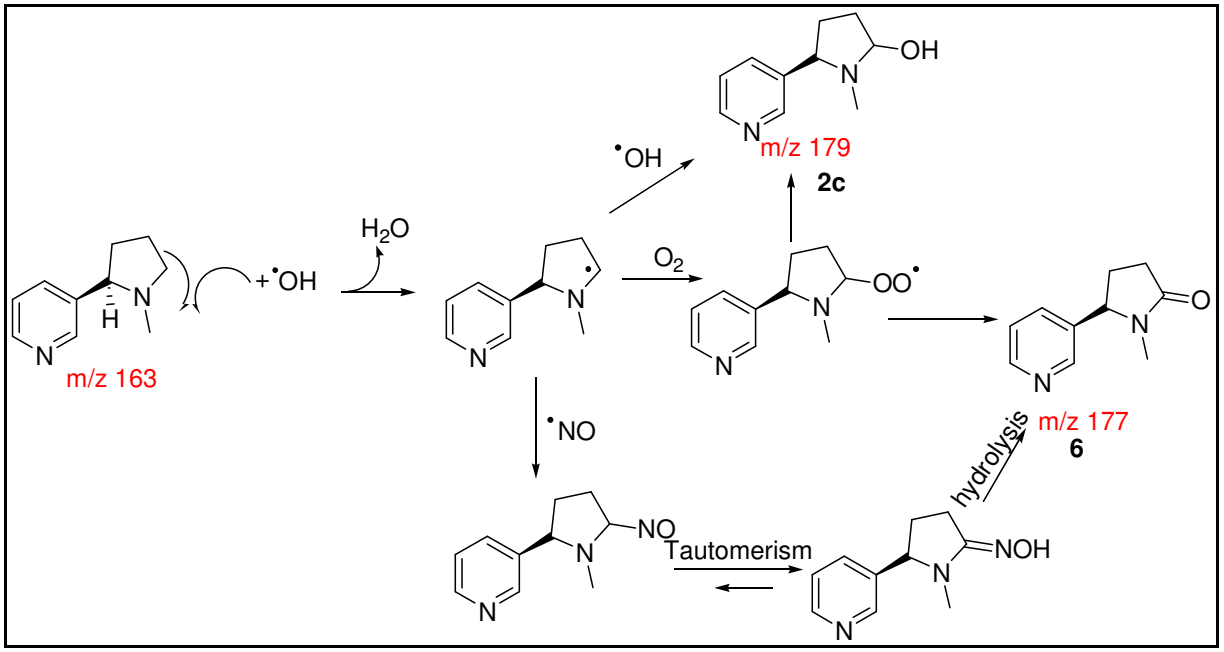

Figure 5: Second proposed reaction mechanism via the hydroxyl radical reactivity in position 2 on the pyrrolidin ring of the Nicotine.

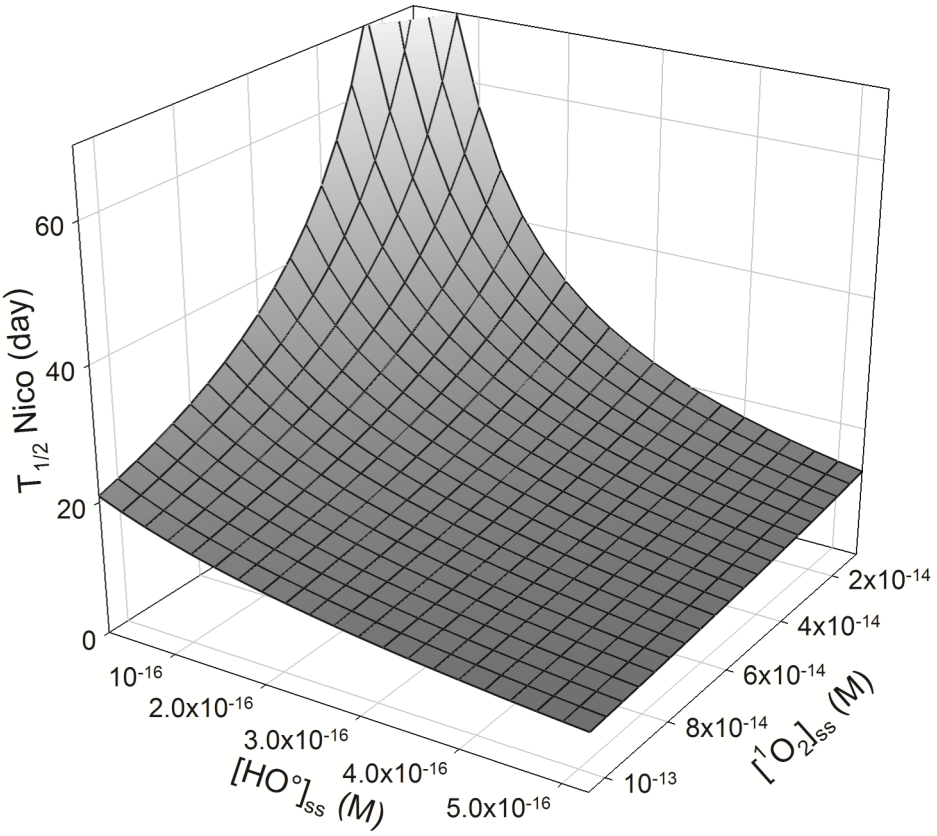

Figure 6: Nicotine half-life time ($T_{1/2}$) assessment considering the reactivity with hydroxyl radical and singlet oxygen. The half-life time value was determined using the second order rate constants obtained in this work and environmental ranges of hydroxyl radical and singlet oxygen from the literature.

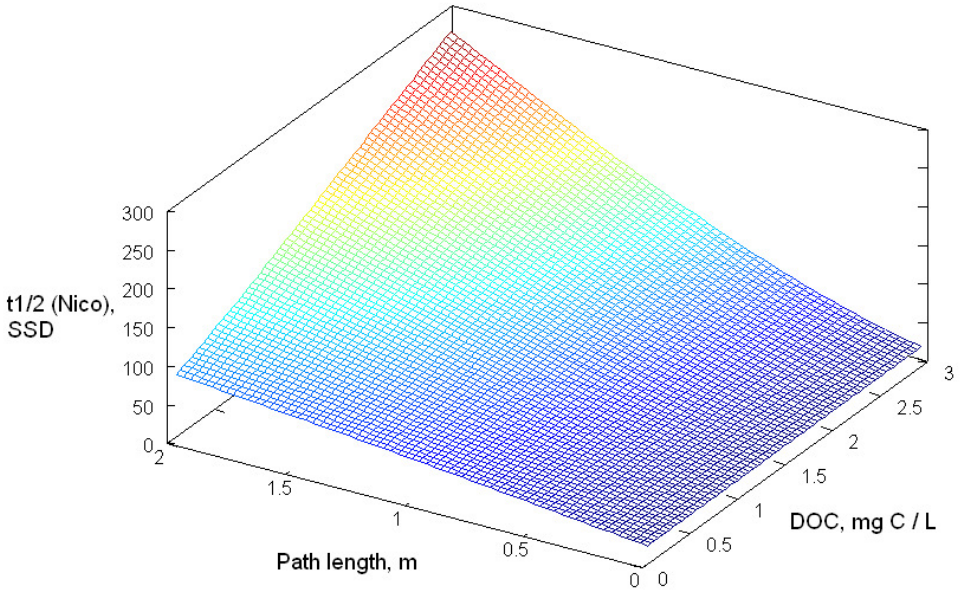

Figure 7. Modelled half-life time of Nico (units of Summer Sunny Days, SSD) as a function a DOC and of the optical path length *l* of sunlight in water. Other water conditions: 0.1 mM nitrate, 1 µM nitrite, 1 mM bicarbonate, 10 µM carbonate (carbonate and bicarbonate are minor $^{\bullet}$OH scavengers; Brezonik and Fulkerson Brekken, 1998).

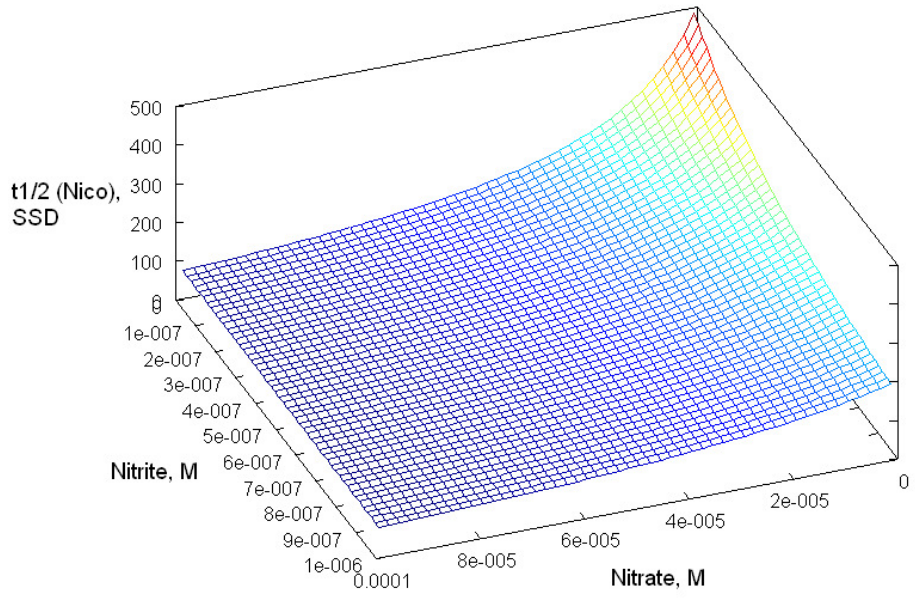

Figure 8. Modelled half-life time of Nico (units of Summer Sunny Days, SSD) as a function a nitrate and nitrite. Other water conditions: l = 1 m, 1 mg C L^{-1} DOC, 1 mM bicarbonate, 10 µM carbonate.